Polypeptide/Multiwalled Carbon Nanotube Hybrid Complexes Stabilized Through Noncovalent Bonding Interactions

Yung-Chih Lin, Shiao-Wei Kuo

Department of Materials and Optoelectronic Science, Center for Nanoscience and Nanotechnology, National Sun Yat-Sen University, Kaohsiung 80424, Taiwan
Correspondence to: S.-W. Kuo (E-mail: kuosw@faculty.nsysu.edu.tw)

Received 10 September 2013; accepted 23 October 2013; published online 18 November 2013
DOI: 10.1002/pola.27000

ABSTRACT: In this study, we used click chemistry to synthesize new linear polypeptide-*g*-pyrene polymers from a mono-azido-functionalized pyrene derivative (N_3-Py) and several poly(γ-propargyl-L-glutamate) (PPLG) oligomers. Incorporating the pyrene units as side chains enhanced the α-helical conformations of these PPLG oligomers in the solid state, as determined using Fourier transform infrared (FTIR) spectroscopy; it also increased the temperature stability of the α-helical secondary structures of the grafted PPLG oligomers, relative to those of the pure PPLG species, as revealed through temperature-dependent FTIR spectroscopic analyses. In addition, the thermal properties of the PPLG-*g*-Py polypeptides (e.g., glass transition temperatures increased by ca. 100 °C) were superior to those of pure PPLG oligomers. Mixing the PPLG-*g*-Py oligomers with multiwalled carbon nanotubes (MWCNTs) in dimethylformamide led to the formation of highly dispersible PPLG-*g*-Py/MWCNT organic/inorganic hybrid complex materials. Fluorescence emission spectra revealed significant π–π stacking between the PPLG-*g*-Py oligomers and the MWCNTs in these complexes. © 2013 Wiley Periodicals, Inc. J. Polym. Sci., Part A: Polym. Chem. **2014**, *52*, 321–329

KEYWORDS: biomaterials; carbon tube; nanotechnology; polypeptides; thermal property

INTRODUCTION Polypeptides are interesting materials because of their close relationship with proteins: they can form hierarchically ordered structures containing α-helices, which can be regarded as a rigid rods stabilized through intramolecular hydrogen bonding interactions, and β-sheets, stabilized by intermolecular interactions, as fundamental secondary motifs.[1,2] Performing conformational studies of model polypeptides is a necessary step toward mimicking the biological activity of more complex proteins.[3,4]

The study of polypeptides has often focused on block copolymers featuring organic nonpolypeptide block segments for tissue engineering and drug delivery applications[5–15]; these block segments have included poly(ethylene oxide),[16] poly(ε-caprolactone),[17] poly(*N*-isopropyl acrylamide),[18] and poly(2-ethyl-2-oxazoline).[19] In the previous studies, we combined polyhedral oligomeric silsesquioxane (POSS) derivatives, inorganic nanoparticles having well-defined macromolecular architectures, with polypeptides to generate polymeric building blocks substituted at the chain end [POSS-*b*-poly(γ-benzyl-L-glutamate) (PBLG)][20–22] or on the side chains [poly(γ-propargyl-L-glutamate) (PPLG)-*g*-POSS].[23,24] We found that the incorporation of POSS units at the chain end or side chains of a polypeptide moiety enhanced its α-helical conformation in the solid state, as determined using Fourier transform infrared (FTIR) spectroscopy, solid-state nuclear magnetic resonance (NMR) spectroscopy, and wide-angle X-ray diffraction analyses. In addition to polypeptide/POSS nanocomposites,[20–24] the covalent surface functionalization of carbon nanotubes (CNTs) with polypeptides has also received much recent attention for its biological applications.[25] For example, Yao et al.[26] proposed a "graft-from" approach to synthesize polypeptide-modified multiwalled carbon nanotubes (MWCNTs); the MWCNTs were first amino-functionalized and then used as initiators to form PBLG-MWCNTs through ring-opening polymerization (ROP) of the monomer γ-benzyl-L-glutamate *N*-carboxyanhydride (BLG-NCA). In addition, Tang and Zhang[27] used amino-functionalized single-walled carbon nanotubes (SWCNTs) as initiators to synthesize grafted PBLG polymers through ROP of the BLG-NCA. Tang et al.[28] proposed another "graft-to" method for the synthesis of polypeptide-modified SWCNTs through addition reactions using azido-terminated PBLG derivatives. Such covalent functionalization of CNTs, however, often changes the hybridization of the carbon atoms from sp^2 to sp^3, potentially deteriorating the optical, electronic, and mechanical properties. Noncovalent approaches toward the functionalization of CNTs, without destroying their

Additional Supporting Information may be found in the online version of this article.

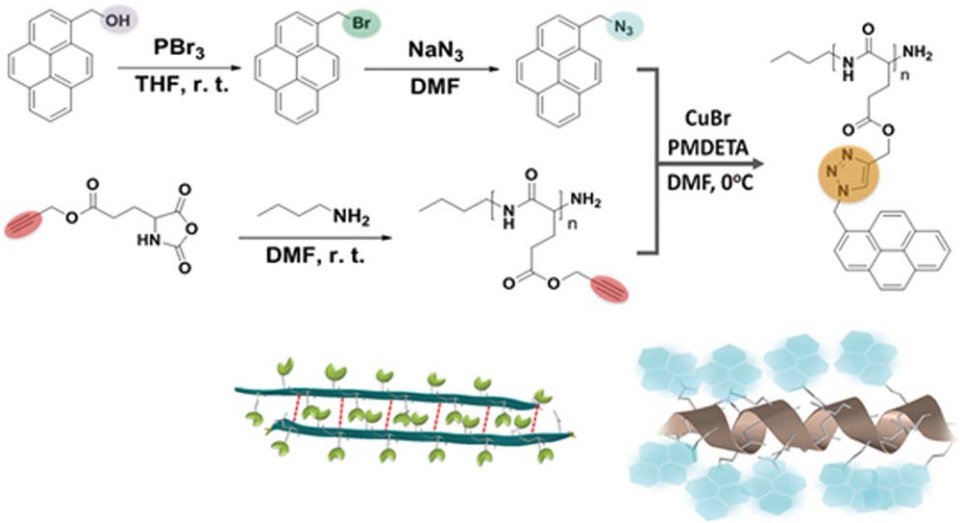

SCHEME 1 Synthesis of PPLG-*g*-Py polypeptides. [Color figure can be viewed in the online issue, which is available at wileyonlinelibrary.com.]

electronic configurations, can enhance their dispersibility while maintaining their electronic and mechanical properties. Tang and Zhang[29] demonstrated that SWCNTs can be dispersed homogeneously through π–π stacking with a chain end-modified pyrenyl-PBLG derivative, taking advantage of the ability of pyrene groups to form strong π–π interactions with CNT surfaces.

If a pyrene moiety is located only at the chain end of a polypeptide, then the amount of pyrene in a sample would be extremely low and less effective at stabilizing a CNT. Therefore, in this study, we linked pyrene moieties to the side chains of a polypeptide and investigated the effects of such grafting on the self-assembly and secondary structures of the polypeptide. First, we prepared PPLG oligomers with different degrees of polymerization (DP) through ROP of γ-propargyl-L-glutamate *N*-carboxyanhydride (PLG-NCA), using butylamine as the macroinitiator. Next, we synthesized PPLG-*g*-Py polypeptides through click reactions (Scheme 1) with an azido-functionalized pyrene derivative (N_3-pyrene). We characterized the secondary structures of PPLG and PPLG-*g*-Py using FTIR spectroscopy and investigated the interactions and dispersibility of MWCNTs and PPLG-*g*-Py using fluorescence spectroscopy and transmission electron microscopy (TEM).

EXPERIMENTAL

Materials

Phosphorus tribromide (PBr_3) was purchased from Acros. Propargyl alcohol and L-glutamic acid were purchased from Tokyo Kasei Kogyo. Copper(I) bromide (CuBr) was purified by washing with glacial AcOH overnight, followed by washing with absolute EtOH and Et_2O, and then drying under vacuum. 1-Pyrenemethanol (OH-Py), *N*,*N*-dimethylformamide (DMF), sodium azide (NaN_3), and *N*,*N*,*N*′,*N*″,*N*″-pentamethyldiethylenetriamine (PMDETA, 99%) were purchased from Aldrich. All solvents were distilled prior to use. PPLG was prepared according to a previously reported procedure.[23,30]

Bromomethylpyrene (Br-Py)

A solution of OH-Py (3.00 g, 12.9 mmol) and PBr_3 (1.41 mL, 15.0 mmol) in dry tetrahydrofuran (THF, 10.0 mL) was stirred at room temperature for 30 min under Ar. After filtering, the residue was washed several times with Et_2O. The resulting product was filtered off and dried under vacuum at room temperature (2.67 g, 70%).

^{1}H NMR ($CDCl_3$): $\delta = 8.35$–7.97 (m, 9H), 5.21 (s, 2H). ^{13}C NMR ($CDCl_3$): $\delta = 32.18$, 122.73, 124.53, 124.77, 125.01, 125.53, 125.56, 126.19, 127.24, 127.60, 127.94, 128.14, 128.97, 130.46, 130.68, 131.12, 131.86 (Supporting Information Figs. S2 and S3).

Azidomethylpyrene (N_3-Py)

NaN_3 (1.00 g, 15.4 mmol) was added to a solution of Br-Py (1.50 g, 5.08 mmol) in DMF (20 mL) and then the mixture was heated at 60 °C for 8 h under Ar. The solution was cooled to room temperature, diluted with Et_2O (100 mL), and washed with 1 M of $NaHCO_3$ (2 × 50 mL) and water (2 × 50 mL). The organic phase was dried ($MgSO_4$) and concentrated under vacuum to yield a yellowish solid (1.18 g, 90%).

^{1}H NMR ($CDCl_3$): $\delta = 8.25$–7.95 (m, 9H), 5.01 (s, 2H). ^{13}C NMR ($CDCl_3$): $\delta = 32.18$, 122.61, 124.58, 124.98, 125.50, 125.57, 126.13, 127.26, 127.39, 127.82, 128.19, 128.32, 129.18, 130.66, 131.16, 131.71 (Supporting Information Figs. S2 and S3).

PPLG, Through ROP of PLG-NCA

PLG-NCA was frozen under vacuum using liquid N_2. DMF was added via syringe and then the resulting solution was warmed to 0 °C and N_2 gas was added to fill the reactor. Butylamine, the initiator, was added and the mixture was stirred for 48 h at 0 °C. The solvent was evaporated under vacuum and then the solid residue was dissolved in DMF

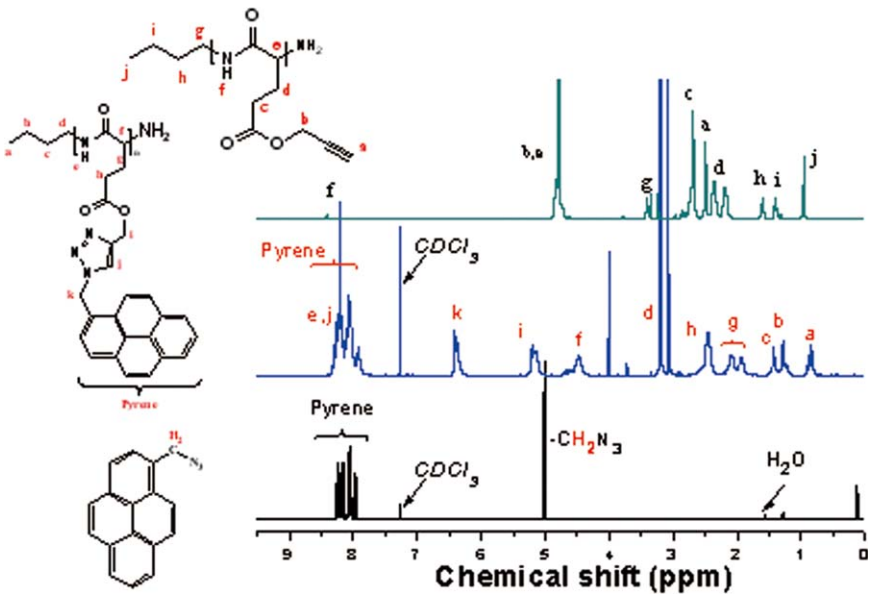

FIGURE 1 ^{1}H NMR spectra of $PPLG_5$, N_3-Py, and $PPLG_5$-*g*-Py polypeptides. [Color figure can be viewed in the online issue, which is available at wileyonlinelibrary.com.]

and precipitated with cold Et_2O or MeOH. The polymer was filtered off and dried under vacuum at room temperature.

Poly(γ-propargyl-L-glutamate)-*g*-Py

N_3-Py (0.60 g, 2.33 mmol), PPLG (0.20 g, 1.198 mmol), and CuBr (0.17 g, 1.180 mmol) were dissolved in DMF (30 mL) in a flask equipped with a magnetic stirrer bar. After one brief freeze/pump/thaw cycle, PMDETA (24.6 μL, 1.18 mmol) was added. The reaction mixture was then carefully degassed through three freeze/pump/thaw cycles, placed in an oil bath thermostated at 60 °C, and stirred for 24 h. After evaporating the solvent under reduced pressure, the residue was dissolved in THF and passed through a neutral alumina column to remove the copper catalyst. The concentrated THF solvent was evaporated, and the product precipitated using MeOH. The resulting solid was filtered off and dried under vacuum at room temperature, yielding a yellowish powder.

PPLG-*g*-Py/MWCNT Complexes

Supramolecular complexes of PPLG-*g*-Py and MWCNTs were prepared via solution blending as follows: A dispersion of 1 mg of MWCNTs in 5 mL of DMF was sonicated for 1 h and then the dispersed solution was added to a solution containing 50 mg of PPLG-*g*-Py in 5 mL of DMF. The mixture was sonicated for an additional 1 h, followed by centrifuge at 5000 rpm for 90 min. The residue was collected by filtration and washed thoroughly with DMF (more than five times) until the filtrate was no longer fluorescent when irradiated with UV light (365 nm), indicating that all excess free polymer had been removed and dried at 30 °C under vacuum for 24 h.

Characterization

^{1}H and ^{13}C NMR spectra were recorded at room temperature using a Bruker AM 500 (500 MHz) spectrometer, with the residual proton resonance of the deuterated solvent acting as the internal standard. Molecular weights and molecular weight distributions were determined through gel permeation chromatography using a Waters 510 high-performance liquid chromatography system equipped with a 410 differential refractometer and three Ultrastyragel columns (100, 500, and 10^3 Å) connected in series, with DMF as the eluent (flow rate, 0.4 mL/min). Thermal analysis through differential scanning calorimetry (DSC) was performed using a TA-Q20 instrument operated at a scan rate of 10 °C/min over the temperature range from −90 to +200 °C under a N_2 atmosphere. FTIR spectra of the polymer films were recorded using the conventional KBr disk method. The films used in this study were sufficiently thin to obey the Beer–Lambert law. FTIR spectra were recorded using a Bruker Tensor 27 FTIR spectrophotometer; 32 scans were collected at a spectral resolution of 1 cm^{-1}. As polymers containing amide groups are hygroscopic, pure N_2 gas was used to purge the spectrometer's optical box to maintain dry sample films. Mass spectra were recorded using a BrukerDaltonicsAutoflex III MALDI-TOF mass spectrometer with the following voltage parameters: ion source 1, 19.06 kV; ion source 2, 16.61 kV; lens, 8.78 kV; reflector 1, 21.08 kV; reflector 2, 9.73 kV. TEM images were recorded using a JEOL-2100 transmission electron microscope operated at an accelerating voltage of 200 kV.

RESULTS AND DISCUSSION

Synthesis of Pyrene-grafted Polypeptides (PPLG-*g*-Py)

Figure 1 shows the ^{1}H NMR spectra of N_3-Py, PPLG-*g*-Py, and PPLG. The signal of the methylene group of N_3-Py (5.01 ppm) shifted downfield significantly relative to the corresponding signal of PPLG-*g*-Py (6.41 ppm), as did the signal of the methylene units of the propargyl groups of PPLG

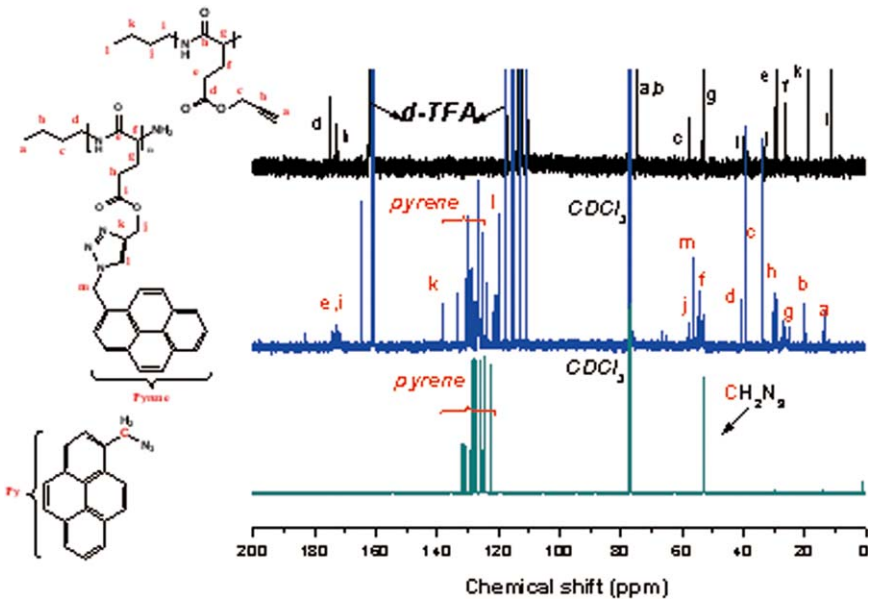

FIGURE 2 ^{13}C NMR spectra of $PPLG_5$, N_3-Py, and $PPLG_5$-*g*-Py polypeptides. [Color figure can be viewed in the online issue, which is available at wileyonlinelibrary.com.]

(4.80 ppm) after forming the corresponding methylene units in PPLG-*g*-Py (5.18 ppm). In addition, the signals for the pyrene moiety also appeared in the spectrum of PPLG-*g*-Py. The sharp resonance at 7.90 ppm was owing to the protons of the triazole structures that resulted from the click reactions, confirming the successful synthesis of the PPLG-*g*-Py polypeptides. Figure 2 shows the ^{13}C NMR spectra of N_3-Py, PPLG-*g*-Py, and PPLG. The signals of the carbon atoms of the ester and amide units of PPLG-*g*-Py appeared at 173.0 and 174.1 ppm, respectively; those of the pyrenyl aromatic ring of N_3-Py appeared at 124.0, 125.0, 126.3, 126.7, 128.3, 129.2, 129.4, 130.1, 130.8, and 133.3 ppm. The signal for the methylene group of N_3-Py (53.0 ppm) shifted downfield significantly relative to the corresponding signal (56.1 ppm) for the PPLG-*g*-Py polypeptides. The signals for the ester carbon atom (**C**-j) and the amino acid α-carbon atoms (NHCO**C**) appear at 57.4 and 54.3 ppm (α-helical conformation), respectively. The signal of the alkyne carbon atoms of PPLG (originally at 73.4 ppm) disappeared, but two new peaks appeared—at 121.4 and 138.2 ppm—representing the carbon atoms of the triazole structures that resulted from the click reactions, thereby confirming the synthesis of PPLG-*g*-

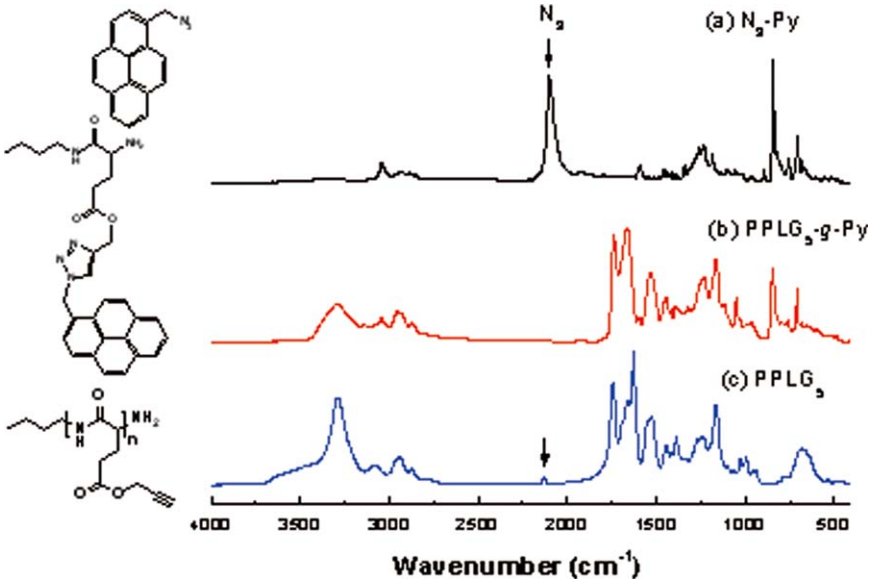

FIGURE 3 FTIR spectra of (a) N_3-Py, (b) $PPLG_5$-*g*-Py, and (c) $PPLG_5$. [Color figure can be viewed in the online issue, which is available at wileyonlinelibrary.com.]

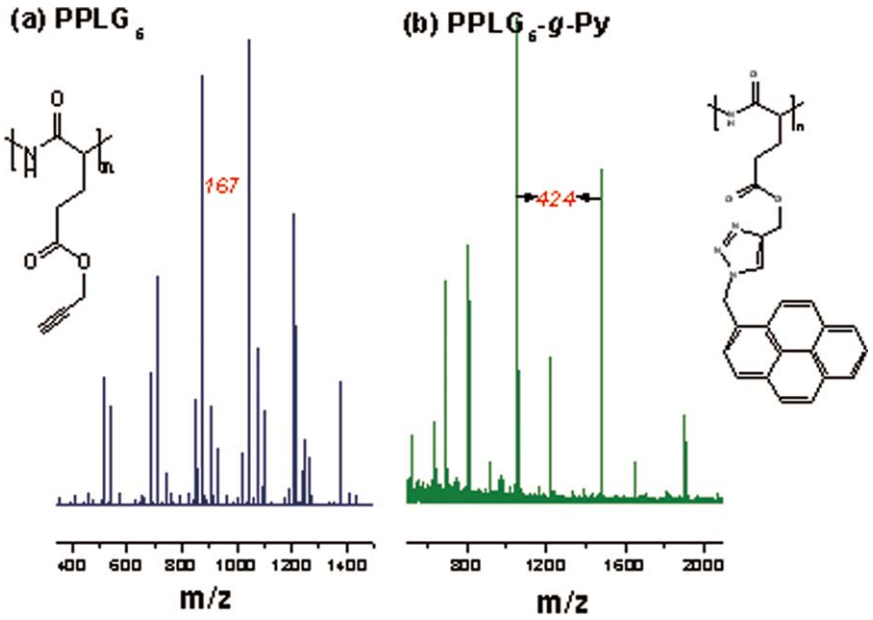

FIGURE 4 MALDI-TOF mass spectra of the oligopeptides (a) $PPLG_5$ and (b) $PPLG_5$-*g*-Py. [Color figure can be viewed in the online issue, which is available at wileyonlinelibrary.com.]

Py. Figure 3 shows the complete disappearance of the characteristic signals for the azido and acetylene groups in the FTIR spectra of the product grafter polypeptides. The signal at 2100 cm^{-1}, corresponding to the absorbance of the azido group of N_3-Py, and the signal at 2130 cm^{-1}, corresponding to the acetylene groups of PPLG, were absent in the spectra of the PPLG-*g*-Py oligomers. The absorption bands of the pyrene units at 846, 1589, and 1602 cm^{-1} and the amide I groups of PPLG at 1655 cm^{-1} were also evident in the spectra of the PPLG-*g*-Py-grafted systems, indicating that it was only the azido and acetylene functionalities that had participated in the click reactions. The well-defined structure was confirmed in the corresponding MALDI-TOF MS spectra (Fig. 4), which revealed only one apparent distribution for both PPLG and PPLG-*g*-Py. The mass differences between all adjacent pairs of peaks were *m/z* 167 for PPLG and *m/z* 424 for PPLG-*g*-Py, as expected for the repeating units of PPLG and PPLG-*g*-Py, respectively. Taken together, the data from the ^1H and ^{13}C NMR, FTIR, and MALDI-TOF MS spectra all confirmed the successful syntheses of the pyrene fluorophore-containing polypeptides (PPLG-*g*-Py) and the results are summarized in Table 1.

TABLE 1 Characterizations of PPLG-*g*-Py Used in this Study

Polymers	M_n[a]	M_n[b]	PDI[b]
$PPLG_5$	910	3,090	1.07
$PPLG_{30}$	5,080	6,890	1.13
$PPLG_5$-Py	2,190	2,960	1.07
$PPLG_{30}$-Py	12,790	11,870	1.16

[a] Determined from ^1H NMR spectra.
[b] Determined from GPC analysis.

Thermal Analyses of Pyrene-grafted Polypeptides (PPLG-*g*-Py)

Figure 5 shows DSC thermograms of the PPLG and PPLG-*g*-Py polypeptides. During the second heating run of each of these systems, we observed only one glass transition temperature (T_g, at ca. 20 °C), which increased slightly upon increasing the DP of the pure PPLG.[23] After grafting the pyrene moieties onto the PPLG oligomers, we observed a dramatic change in the second heating run of the DSC analyses. The T_gs of the PPLG-*g*-Py oligomers increased significantly to approximately 117 °C—that is, they were greater than those of the PPLG oligomers by approximately 97 °C. The values also

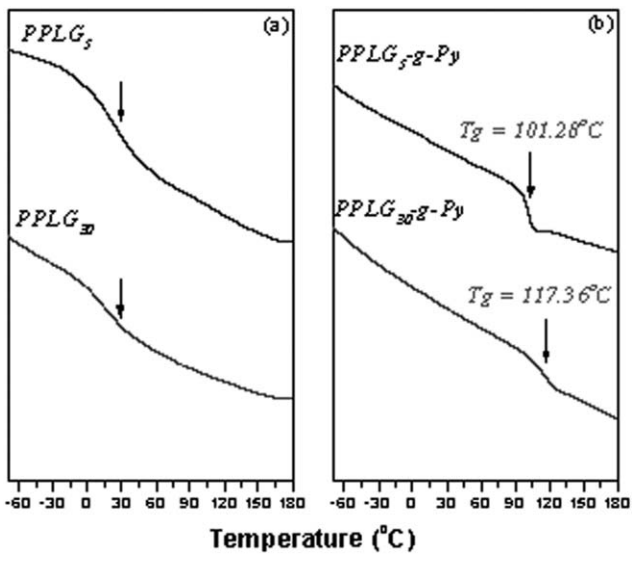

FIGURE 5 DSC traces (second heating runs) of the polypeptides (a) PPLG and (b) PPLG-*g*-Py.

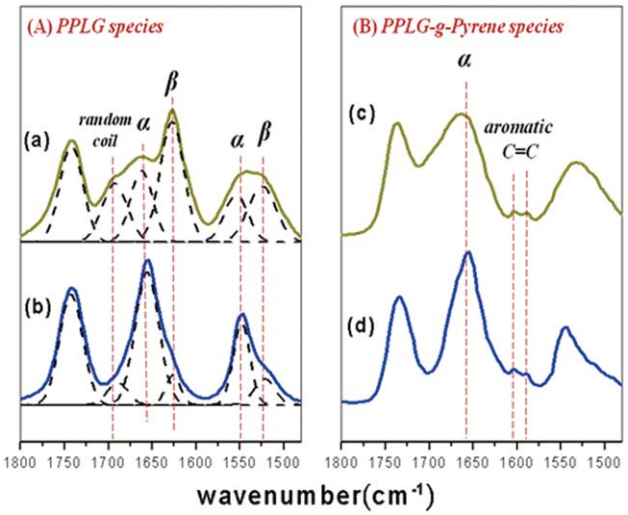

FIGURE 6 FTIR spectra of (A) the PPLG species (a) $PPLG_5$ and (b) $PPLG_{30}$ and (B) the PPLG-*g*-Py species (c) $PPLG_5$-*g*-Py and (d) $PPLG_{30}$-*g*-Py. [Color figure can be viewed in the online issue, which is available at wileyonlinelibrary.com.]

increased slightly upon increasing the DP of the PPLG-*g*-Py-grafted oligomers. The significant increases in the values of T_g of the PPLG-*g*-Py species were owing to the effects of π–π stacking and the rigid aromatic structures of the pyrene moieties, which effectively restricted the chain motion of the PPLG segments, a situation similar to that we had noted after the modification of oligopeptides with POSS nanoparticles.[23,24,31]

Conformations of the Peptide Segments

We recorded FTIR spectra at room temperature to obtain information about the conformations of the peptide segments of the PPLG and PPLG-*g*-Py oligomers (Fig. 6). Analysis of these spectra using the second-derivative technique[4] indicated that the amide I band at 1655 cm^{-1} was characteristic of α-helical secondary structures. For polypeptides possessing a *β*-sheet conformation, the amide I band would have shifted to 1627 cm^{-1}; random coil or turn populations would feature a band located at 1693 cm^{-1}. The signal of the free C═O groups of the side chains of PPLG appeared at 1740 cm^{-1} [Fig. 6(A)], with the signals at 1589 and 1602 cm^{-1} corresponding to stretching of the aromatic rings of the pyrene units of the side chains [Fig. 6(B)]. Next, we used the deconvolution technique to obtain a series of Gaussian distributions to quantify the fraction of each peak [inset, Fig. 6(A)]. The fraction of α-helical secondary structures increased upon increasing the DP of the PPLG oligopeptides; this result is similar to that reported by Papadopoulos et al.[32] for PBLG. At low DPs (<18), both secondary structures were present, but as the DP increased, the α-helical secondary structure was favored. In addition, all of our grafted PPLG-*g*-Py species obtained after performing the click reactions possessed α-helical secondary structures, even those having a relatively low DP (e.g., $PPLG_5$-*g*-Py). This behavior is different from that observed previously for Py-*b*-$PBLG_9$, where the Py unit was located only on the terminus of the polypeptide; because the amount of pyrene in this polypeptide was extremely low, Py-*b*-$PBLG_9$ possessed an α-helical conformation of only 35.0%.[29] Jeon et al.[33] reported that the mobility of the side chains of polyglutamates affects their α-helical conformations; their experimental data revealed that longer, flexible side chains induced weaker hydrogen bonds between the ester C═O groups and the amide linkages in the α-helical conformation. Thus, we suspect that the rigid pyrene moieties enhanced the strength of the hydrogen bonds between the ester C═O groups and the amide linkages in the α-helical conformation, similar to the behavior in grafted PPLG-*g*-POSS species.[23]

We also recorded temperature-dependent FTIR spectra to obtain information relating to the conformations of the peptide segments. Figure 7 shows the FTIR spectroscopic data for $PPLG_5$ and $PPLG_5$-*g*-Py. The amide I and amide II bands appeared at 1655 and 1545 cm^{-1}, respectively, in the α-helical secondary structure; they shifted to 1626 and 1520 cm^{-1}, respectively, in the *β*-sheet conformation. Here, we chose to examine the $PPLG_5$ oligomer because it possessed both α-helical and *β*-sheet conformations; the longer $PPLG_{30}$ oligomer adopted the α-helical secondary structure almost entirely, making it insensitive to changes in temperature. The spectra of $PPLG_5$-*g*-Py indicated that the α-helical secondary structure was stabilized significantly upon attachment of the rigid pyrene units, relative to the FTIR spectra of the PPLG homopeptide. The fraction of α-helical secondary structures of $PPLG_5$ decreased significantly upon increasing the temperature [Fig. 7(A)]; in contrast, the secondary structure of PPLG-*g*-Py remained almost unchanged [Fig. 7(B)]. Thus, the DP, the temperature, and the presence of pyrene moieties all had a strong influence on the stability of the secondary structure. Increasing the DP of all of the polypeptides and attaching pyrene units both led to stabilization of the α-helical secondary structures with respect to increasing temperatures.

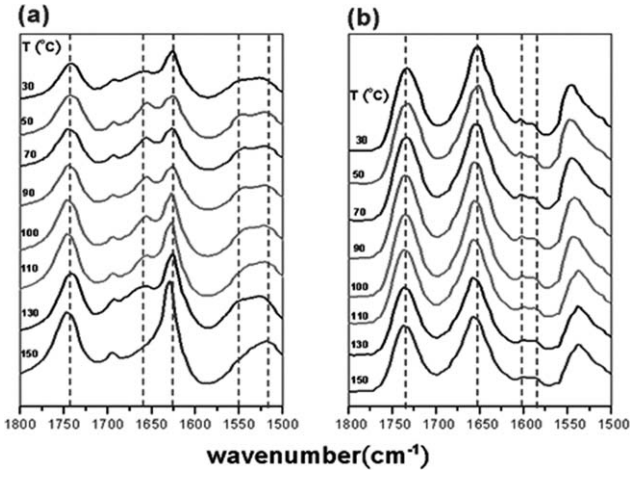

FIGURE 7 FTIR spectra of the oligopeptides (a) $PPLG_5$ and (b) $PPLG_5$-*g*-Py at various temperatures.

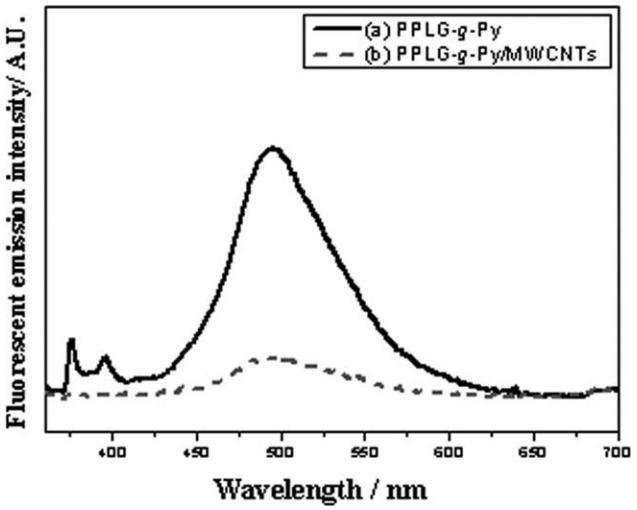

FIGURE 8 PL spectra of PPLG-*g*-Py/MWCNT hybrid complexes.

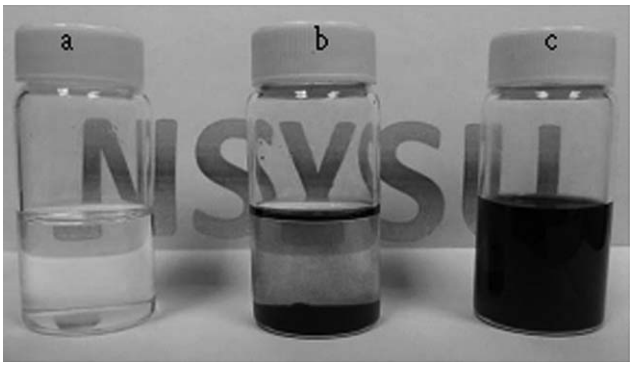

FIGURE 9 Photograph of (a) pure PPLG-*g*-Py polypeptides, (b) pristine MWCNTs, and (c) PPLG-*g*-Py/MWCNT hybrid complexes in DMF (each 1 mg/mL).

PPLG-*g*-Py/MWCNT Complexes Stabilized Through π–π Interactions

Figure 8 shows fluorescence spectra (UV spectra in Supporting Information Fig. S4) of the PPLG-*g*-Py oligomers and the PPLG-*g*-Py/MWCNT complexes in solution after excitation at 343 nm. The spectra for PPLG-*g*-Py exhibited strong fluorescence signals for both monomeric (374 nm) and dimeric (493 nm) pyrene units; the spectra of the PPLG-*g*-Py/MWCNT complexes exhibited very weak excimer fluorescence and quenched monomer fluorescence.[34,35] These findings suggest that most of the pyrene moieties of the PPLG polymers interacted with the MWCNTs through π–π stacking, with only a few of them available for excimer formation as a result of steric hindrance; therefore, our proposed model consists of coexisting PPLG-*g*-Py oligomers (Py/Py excimer) and PPLG-*g*-Py/MWCNT nanohybrids. Scheme 2 shows possible mechanisms of formation and structures determined from fluorescence spectroscopic analyses. Figure 9 shows photographs of DMF solutions of the pure MWCNTs, the pure PPLG-*g*-Py oligomers, and the PPLG-*g*-Py oligomers in the presence of the MWCNTs. The pure PPLG-*g*-Py oligopeptides formed a clear solution, whereas the pure MWCNTs precipitated completely; the addition of the PPLG-*g*-Py oligomers into the suspension of the MWCNTs resulted in a clear brown solution, indicating that soluble complexes were formed as a result of noncovalent interactions (primarily π–π stacking). Supporting Information Figure S5 shows TGA analyses of pristine MWCNT, pure $PPLG_{30}$-*g*-Py polypeptide, and $PPLG_{30}$-*g*-Py/MWCNT hybrid complexes. At 600 °C, we observed most of the pure $PPLG_{30}$-*g*-Py polypeptide is about 20 wt % char yield, and the compounds of pristine MWCNT and $PPLG_{30}$-*g*-Py/MWCNT hybrid complexes were 95.9 and 62.6 wt % char yield, respectively. If a similar weight-loss behavior of pure $PPLG_{30}$-*g*-Py polypeptide and pristine MWCNT is assumed to take place in the hybrid complexes, then the pure $PPLG_{30}$-*g*-Py polypeptide content in the hybrid complexes can be roughly estimated by TGA analysis and to be 33.2 wt %. We used TEM to further investigate the morphologies of dispersions of the pristine MWCNTs and the PPLG-*g*-Py/MWCNT hybrid complexes in EtOH (each at 10^{-3} g/mL) after ultrasonic vibration. Figure 10(a) shows that the

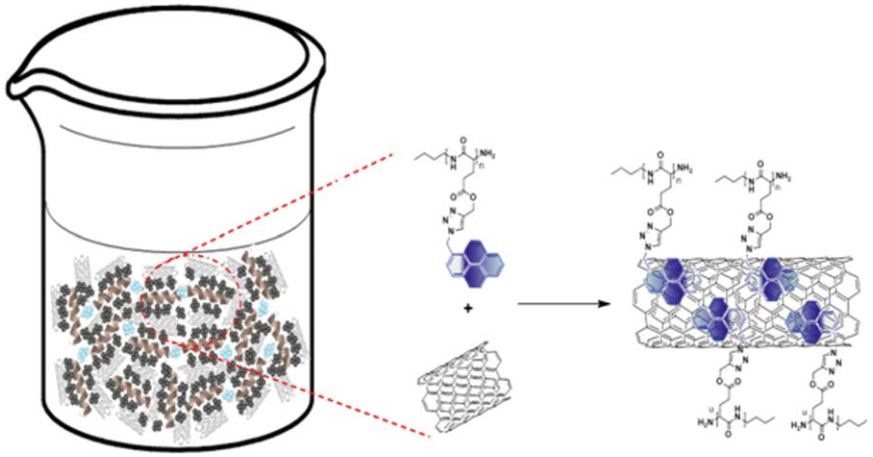

SCHEME 2 Preparation of PPLG-*g*-Py/MWCNT hybrid complexes stabilized through π–π interactions. [Color figure can be viewed in the online issue, which is available at wileyonlinelibrary.com.]

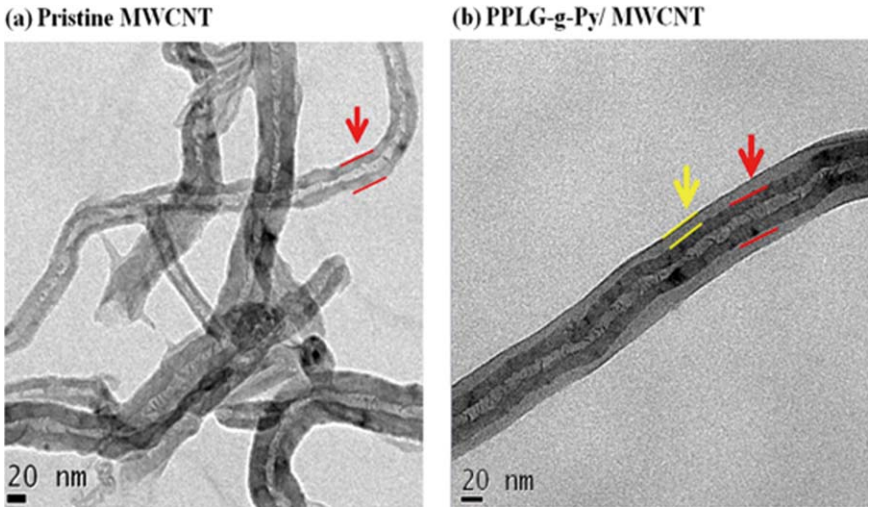

FIGURE 10 Typical TEM images of (a) pristine MWCNTs and (b) PPLG-*g*-Py/MWCNT hybrid complexes. [Color figure can be viewed in the online issue, which is available at wileyonlinelibrary.com.]

pristine MWCNTs exhibited a high degree of aggregation, a result of very strong van der Waals attraction among the CNTs along their fiber axes; in other words, self-aggregation of the CNTs is thermodynamically favored. On the basis of spontaneous formation of polypeptide hybrid complexes through π–π stacking with the MWCNTs, Figure 10(b) shows a uniform dispersion of the MWCNTs within the PPLG-*g*-Py matrix.

CONCLUSIONS

We have prepared a series of new fluorescent PPLG-*g*-Py polymers through ROP of PLG-NCA followed by click reactions with a monofunctional azide-derivatized pyrene. After grafting the pyrene fluorophore units onto the side chains of the PPLG oligopeptides, the fraction of α-helical secondary structures of the PPLG backbones increased as a result of enhanced intramolecular hydrogen bonding induced by the presence of the rigid and bulky pyrene moieties. The thermal properties of the grafted PPLG-*g*-Py systems were superior (increased values of T_g) to those of the pure PPLG oligomers. In addition, noncovalent interactions among the pyrene units of the PPLG-*g*-Py oligopeptides and MWCNTs in DMF solution allowed us to form dispersions in the presence of PPLG-*g*-Py/MWCNT complexes as organic/inorganic nanohybrid materials. Fluorescence emission spectra confirmed the presence of significant π–π interactions among the PPLG-*g*-Py oligopeptides and the MWCNTs.

ACKNOWLEDGMENTS

This study was supported financially by the National Science Council, Taiwan, Republic of China, under contracts NSC 100–2221-E-110-029-MY3 and NSC 102-2221-E-110-008-MY3. The authors thank Hsien-Tsan Lin of the Regional Instruments Center at National Sun Yat-Sen University for help with the TEM experiments.

REFERENCES AND NOTES

1 H. A. Klok, S. Lecommandoux, *Adv. Mater.* **2001**, *13*, 1217–1229.

2 G. J. M. Habraken, C. E. Koning, A. Heise, *J. Polym. Sci. Part A: Polym. Chem.* **2009**, *47*, 6883–6893.

3 K. Tohyama, W. G. Miller, *Nature* **1981**, *289*, 813–814.

4 A. Sanchez-Ferrer, R. Mezzenga, *Macromolecules* **2010**, *43*, 1093–1100.

5 Q. H. Zhou, J. K. Zheng, Z. H. Shen, X. H. Fan, X. F. Chen, Q. F. Zhou, *Macromolecules* **2010**, *43*, 5367–5646.

6 H. F. Lee, H. S. Sheu, U. S. Jeng, C. F. Huang, F. C. Chang, *Macromolecules* **2005**, *38*, 6551–6558.

7 X. H. He, C. Y. Gao, W. Q. Sun, W. Huang, S. Lin, D. Y. Yan, *J. Polym. Sci. Part A: Polym. Chem.* **2013**, *51*, 1040–1050.

8 J. Rao, Y. Zhang, J. Zhang, S. Liu, *Biomacromolecules* **2008**, *9*, 2586–2593.

9 W. Liu, C. M. Dong, *J. Polym. Sci. Part A: Polym. Chem.* **2011**, *49*, 3491–3498.

10 E. Ibarboure, J. Rodriguez-Hernandez, *J. Polym. Sci. Part A: Polym. Chem.* **2006**, *44*, 4668–4679.

11 H. A. Klok, J. F. Langenwalter, S. Lecommandoux, *Macromolecules* **2000**, *33*, 7819–7826.

12 S. Lecommandoux, M. F. Achard, J. F. Langenwalter, H. A. Klok, *Macromolecules* **2001**, *34*, 9100–9111.

13 J. Jacobs, G. Pound-Lana, B. Klumperman, *Polym. Chem.* **2012**, *3*, 2551–2560.

14 P. Papadopoulos, G. Floudas, I. Schnell, I. Lieberwirth, T. Q. Nguyen, H. A. Klok, *Biomacromolecules* **2006**, *7*, 618–626.

15 Y. You, Y. Chen, C. Hua, C. M. Dong, *J. Polym. Sci. Part A: Polym. Chem.* **2010**, *48*, 709–718.

16 G. Floudas, P. Papadopoulos, H. A. Klok, G. W. M. Vandermeulen, J. Rodriguez-Hernandez, *Macromolecules* **2003**, *36*, 3673–3683.

17 C. Hua, C. M. Dong, Y. Wei, *Biomacromolecules* **2009**, *10*, 1140–1148.

18 C. J. Huang, F. C. Chang, *Macromolecules* **2008**, *41*, 7041–7052.

19 S. W. Kuo, H. F. Lee, F. C. Chang, *J. Polym. Sci. Part A: Polym. Chem.* **2008**, *46*, 3108–3119.

20 S. W. Kuo, H. F. Lee, W. J. Huang, K. U. Jeong, F. C. Chang, *Macromolecules* **2009**, *42*, 1619–1626.

21 S. W. Kuo, H. T. Tsai, *Polymer* **2010**, *51*, 5605–5704.

22 Y. C. Lin, S. W. Kuo, *J. Polym. Sci. Part A: Polym. Chem.* **2011**, *49*, 2127–2137.

23 Y. C. Lin, S. W. Kuo, *Polym. Chem.* **2012**, *3*, 162–171.

24 Y. C. Lin, S. W. Kuo, *Polym. Chem.* **2012**, *3*, 882–891.

25 S. Wang, E. S. Humphreys, S. Y. Chung, D. F. Delduco, S. R. Lustig, H. Wang, K. N. Parker, N. W. Pizzo, S. Subramoney, Y. M. Chiang, A. Jagota, *Nat. Mater.* **2003**, *2*, 196–200.

26 Y. Yao, W. Li, S. Wang, D. Yan, X. Chen, *Macromol. Rapid Commun.* **2006**, *27*, 2019–2025.

27 H. Tang, D. Zhang, *J. Polym. Sci. Part A: Polym. Chem.* **2010**, *48*, 2340–2350.

28 H. Tang, C. U. Lee, D. Zhang, *J. Polym. Sci. Part A: Polym. Chem.* **2011**, *49*, 3228–3238.

29 H. Tang, D. Zhang, *J. Polym. Sci. Part A: Polym. Chem.* **2013**, *51*, 4489–4497.

30 Y. C. Lin, P. I. Wang, S. W. Kuo, *Soft Matter* **2012**, *8*, 9676–9684.

31 D. J. Liaw, K. L. Wang, K. R. Lee, J. Y. Lai, *J. Polym. Sci. Part A: Polym. Chem.* **2007**, *45*, 3022–3031.

32 P. Papadopoulos, G. Floudas, H. A. Klok, I. Schnell, T. Pakula, *Biomacromolecules* **2004**, *5*, 81–91.

33 S. Jeon, J. Choo, D. Sohn, S. N. Lee, *Polymer* **2001**, *42*, 9915–9919.

34 H. Murakami, T. Nomura, N. Nakashima, *Chem. Phys. Lett.* **2003**, *378*, 481–485.

35 K. W. Huang, Y. R. Wu, K. W. Jeong, S. W. Kuo, *Macromol. Rapid Commun.* **2013**, *34*, 1530–1536.